Atom Transfer Radical Copolymerization of Methyl Methacrylate and *n*-Butyl Acrylate

Michael J. Ziegler and Krzysztof Matyjaszewski*

Center for Macromolecular Engineering, Department of Chemistry, Carnegie Mellon University, 4400 Fifth Avenue, Pittsburgh, Pennsylvania 15213

Received July 10, 2000

ABSTRACT: Copolymers of methyl methacrylate and *n*-butyl acrylate were prepared using atom transfer radical polymerization catalyzed by CuBr/4,4′-di(5-nonyl)-2,2′-bipyridine (dNbpy), CuBr/*N*,*N*,*N*′,*N*″,*N*″-pentamethyldiethylenetriamine (PMDETA), and CuBr/tris[2-(dimethylamino)ethyl]amine (Me_6TREN). Point estimates and 95% joint confidence intervals of the reactivity ratios were calculated for the copolymerizations catalyzed by CuBr/dNbpy ($r_{MMA} = 2.52$, $r_{BA} = 0.265$) and those catalyzed by CuBr/PMDETA ($r_{MMA} = 3.15$, $r_{BA} = 0.37$) using previously described least-squares calculations. Semilogarithimic plots of monomer conversion vs time were nearly linear. Plots of M_n vs monomer conversion were linear, and polydispersity decreased with increasing monomer conversion. Copolymerizations were simulated using Predici 5.3.2 in order to better understand the experimentally observed results.

Introduction

The past several years have witnessed significant growth in the field of controlled/living radical polymerization (CRP).[1,2] Atom transfer radical polymerization (ATRP) is one CRP technique in particular that has proven to be very robust and a versatile method for the polymerization of a wide range of monomers.[1−6] Additionally, ATRP has been shown to be effective for the synthesis of well-defined polymers with many different types of architectures and sequential compositions.[7−12] There are also several reports of the use of ATRP to prepare a novel class of materials, gradient copolymers.[13−15]

Gradient copolymers are copolymers in which the instantaneous composition of the polymer changes continuously from one end of the chain to the other.[14−16] As shown in Scheme 1, this is in contrast to block copolymers, which have no change in composition until the crossover from one block to the other, and random copolymers, which have no continuous change in instantaneous composition. To achieve this continuous change in instantaneous composition, all chains must be initiated simultaneously and must survive until the end of the polymerization. Therefore, a living (ionic) or controlled/living radical polymerization technique must be employed, as the significant presence of chain breaking reactions would lead to heterogeneity in composition as well as in molecular weight.

Two types of gradient copolymers can be synthesized: controlled gradients and spontaneous gradients. Controlled gradient copolymers are prepared in semibatch copolymerizations, with controlled addition of one monomer to the other during the course of the polymerization. This results in composition gradients that are manipulated by the forced change in monomer feed composition. Spontaneous gradients are formed in batch copolymerizations, where the significance of the composition gradient is determined exclusively by the reactivity ratios of the monomer pair and the initial monomer feed concentration. Our group has previously reported on the semibatch copolymerizations of styrene/acrylonitrile[17] and styrene/*n*-butyl acrylate,[18] the batch copolymerizations of styrene/acrylonitrile[17] and styrene/*n*-butyl acrylate,[19] and preliminary results for methyl methacrylate/*n*-butyl acrylate[20] using ATRP. Reports from other laboratories have also demonstrated the usefulness of ATRP in the synthesis of gradient or statistical copolymers.[21−26]

Scheme 1. Schematic Representation of the Composition in Block, Gradient, and Statistical Copolymers, in Which the Open Circles Denote Monomer 1 and the Closed Circles Denote Monomer 2

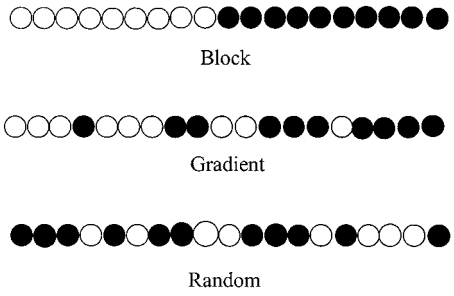

It is the purpose of this paper to compare the results of the ATRP batch copolymerization of methyl methacrylate (MMA) with *n*-butyl acrylate (*n*-BA) using different catalytic systems. It has previously been shown that both of these monomers can be homopolymerized in a controlled fashion by ATRP,[27,28] and we now intend to show that they can also be simultaneously copolymerized in a well-controlled manner using different copper/ligand complexes. This monomer pair is of interest due to the large differences in the monomer reactivity ratios in a free radical process.[24,25,29−33] It is anticipated that this difference will lead to a large spontaneous gradient in instantaneous composition along the growing polymer chain. Living or controlled/living polymerizations will allow the formation of a continuous gradient in composition along the chain, which is in direct contrast with conventional radical polymerization. In conventional radical polymerizations, a large difference in reactivity ratios would lead to one monomer being preferentially consumed first, resulting in polymer chains with high MMA content during the initial stages of the polymerization and polymers with high *n*-BA content at the later stages of the polymerization. In a

10.1021/ma001182k CCC: $20.00
Published on Web 01/03/2001

conventional radical polymerization the differences in reactivity ratios are manifested in a composition drift among a *variable number* of chains, which are created and destroyed during the polymerization. In contrast, composition drift in a controlled radical polymerization manifests itself along the chain and among a *fixed number* of chains formed only at the beginning of the reaction.

This report examines the copolymerization of the monomer pair using several different copper-based catalysts, to compare the behavior of these catalysts and show in all cases that the copolymerizations proceed via the same radical mechanism. For each of the three catalyst systems studied, we have analyzed the kinetic, molecular weight, and cumulative composition behavior of the copolymerization. The reactivity ratios of the monomer pair were also examined for each catalyst system.

In an effort to gain deeper insight into the influence of the ATRP activation/deactivation equilibrium on the modes of propagation and cross-propagation in this copolymerization, we have employed a series of simulated kinetic experiments. Work from this laboratory has previously demonstrated the usefulness of simulations in studying the kinetic behavior of ATRP systems.[34−36] Building on this work, we have studied the influence of kinetic parameters on the concentration of various species in the copolymerizations and compared these results with the experimentally observed behavior of these copolymerizations.

Experimental Section

Materials. Monomers (*n*-BA and MMA) (Acros) were dried over CaH_2 and vacuum-distilled prior to use. Methyl 2-bromopropionate (Aldrich) was vacuum-distilled prior to use, as was PMDETA (Aldrich). The ligand dNbpy was synthesized according to a previously published procedure,[37] as was Me_6-TREN.[38] Copper(I) bromide (Aldrich) was stirred in glacial acetic acid for 12 h, filtered, washed with ethanol, and dried at 100 °C under vacuum for 3 days. The internal standard, 1,4-dimethoxybenzene (Aldrich), was recrystallized from methanol.

Polymerizations. In a typical procedure, solids were added to a 25 mL round-bottom flask equipped with a stirring bar. The flask was evacuated and backfilled with nitrogen three times. The monomers were degassed by sparging with N_2 for 30 min and then added to the reaction flask via syringe. The reaction mixture was heated to the polymerization temperature, and then initiator was added via syringe. In the case of polymerizations with liquid ligands, they were added with the monomers.

Characterization. Conversion was measured using a Shimadzu GC-17A against 1,4-dimethoxybenzene as an internal standard. Molecular weights were measured using a GPC equipped with a Waters 717 Plus autosampler, PSS 10^5, 10^3, 10^2 Å, and guard columns, and a Waters 410 RI detector against polystyrene and poly(methyl methacrylate) standards. Cumulative compositions were calculated from residual monomer feed analysis.

Simulations. Simulations were performed using Predici[39] version 5.3.2. Unless noted otherwise, the parameters used were the ones shown in Table 1. The kinetic parameters given are values estimated for dNbpy at 90 °C based on previous kinetic studies.[28,40] The deactivation rate of MMA was based on the value for styrene due to the similar reactivity of the two monomers, and activation rate was then adjusted accordingly.[41] The initiator used in these simulation was methyl 2-bromopropionate (MBP), which was chosen as a model for acrylate chain ends and was assumed to have the same reactivity as a pBA−Br, except rate constant of addition. It was reported before that due to entropic reasons, low molar mass radicals add to alkenes ∼10 times faster than macromolecular analogues.[42] The termination rate constants used in this work are based on values previously given for the homopolymerization of styrene.[35] The rate constants of termination for styrene, BA, and MMA are similar for the corresponding homo-termination and cross-termination reactions. The ratio of k_{tc} to k_{td} for *n*-BA was assumed to be similar as for styrene. This ratio is probably different, however, in the case of MMA, as MMA radicals are tertiary radicals as opposed to styrene and *n*-BA which are secondary radicals. The homo- and cross-termination rate constants were assumed to be the same. The results of these simulations should not be affected by this assumption, as the percentage of chains that experience termination reactions is low.

Table 1. Kinetic Parameters for Copolymerization of BA with MMA Using CuBr(dNbpy)$_2$/MBP Initiating Systems at 90 °C

parameter	value	parameter	value
k_{act}(MMA)	10^1 L/(mol s)	k_i(BA)	5×10^5 L/(mol s)
k_{deact}(MMA)	10^7 L/(mol s)	k_{tc}[a]	10^9 L/(mol s)
k_{act}(BA)	10^{-1} L/(mol s)	k_{td}[a]	10^8 L/(mol s)
k_{deact}(BA)	8×10^7 L/(mol s)	k_{t0}	5×10^9 L/(mol s)
k_p(MMA)	2.8×10^3 L/(mol s)	k_{tp}[a]	10^9 L/(mol s)
k_p(BA)	5×10^4 L/(mol s)	$[MMA]_0$	4.0 mol/L
k_{BM}	1.5×10^5 L/(mol s)	$[BA]_0$	4.0 mol/L
k_{MB}	9.3×10^2 L/(mol s)	$[MBP]_0$	0.0258 mol/L
k_i(MMA)	1.5×10^6 L/(mol s)	$[Cu(I)]_0$	0.0258 mol/L

[a] The value of the termination rate constants were varied in a chain length dependent manner as was previously described.[35]

The parameters in Table 1 were varied when other catalyst systems were studied. The values used for the PMDETA catalyst system[43] and the Me_6TREN catalyst system[44] are based on previously reported experimental work and are quoted in captions for Figure 14.

Reactivity Ratios and Statistical Methods. Low conversion copolymer composition values calculated from residual feed analysis have large errors and may be biased by preferential initiation of one monomer by the initiating radical. Therefore, extended conversion kinetic data were used (attempting to cover 20−50% conversion range) to estimate monomer reactivity ratios using an integrated form of the composition equation.[19] The "sum-of-squares space" (SS-space) approach was used to calculate joint confidence intervals (JCIs). Full details of the calculations as well as the complete VBA code used to construct the SS-space surface were published as the Supporting Information to ref 19.

Results

As mentioned above, copolymerizations of MMA and *n*-BA were conducted using three different copper-based catalyst systems. The reaction conditions used for the copolymerizations were optimized for each catalyst system in order to minimize side reactions and are listed in Table 2. The conditions used in the copolymerizations with the Me_6TREN catalyst system reflect several of the difficulties experienced with this catalyst. This catalyst has been shown to be very effective for the polymerization of acrylates.[44] It has, however, proven to be a poor choice for the polymerization of methacrylates, due to an overly high radical concentration and the limited solubility of the Cu(II) species in the reaction mixture.[45] In the copolymerization experiments presented in this paper, the catalyst concentration relative to initiator was reduced in the Me_6TREN system, and additional deactivator was added at the beginning of the reaction to reduce the concentration of radicals at the beginning of the reaction. Additionally, the reactions were conducted in 20% ethylene carbonate to further reduce the concentration of radicals, but more importantly to increase the solubility of the Cu(II) deactivating species

Table 2. Reaction Conditions

catalyst system	initiator	$[M]_0:[I]_0:[Cu(I)]_0:[Cu(II)]_0$:[ligand]	temp (°C)	solvent
CuBr/2dNbpy	MBP	300:1:1:0:2	90	bulk
CuBr/PMDETA	MBP	300:1:1:0:1	60	bulk
CuBr/Me_6TREN	MBP	300:1:0.5:0.1:0.6	60	20% (vol to M) ethylene carbonate

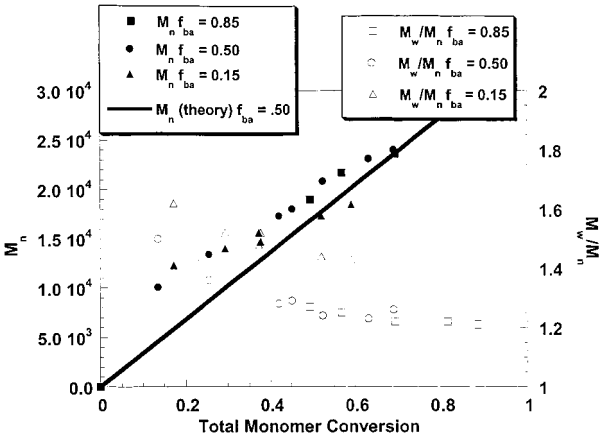

Figure 1. Molecular weight and polydispersity vs total conversion of monomer for the copolymerization of MMA and *n*-BA at several monomer feed conditions, catalyzed by CuBr/2dNbpy. Reaction conditions shown in Table 2.

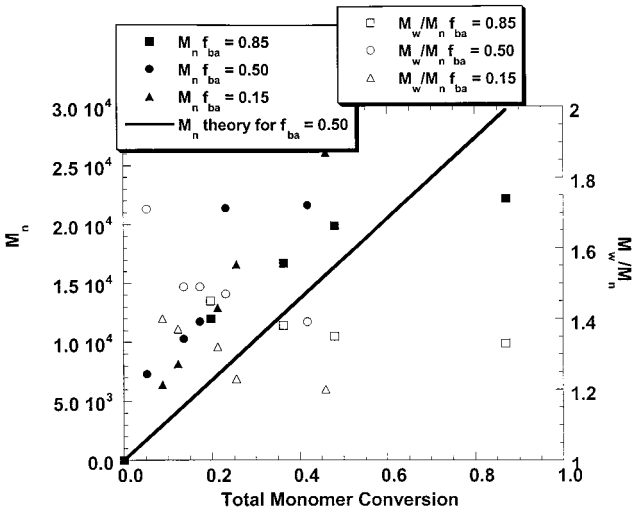

Figure 2. Molecular weight and polydispersity vs total conversion of monomer for the copolymerization of MMA and *n*-BA at several monomer feed conditions, catalyzed by CuBr/PMDETA. Reaction conditions shown in Table 2.

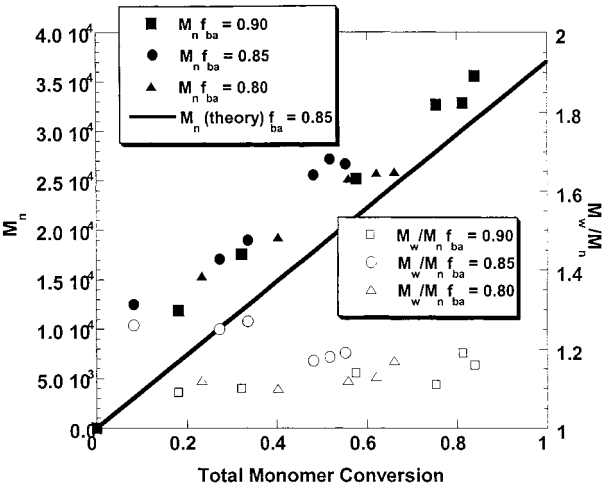

Figure 3. Molecular weight and polydispersity vs total conversion of monomer for the copolymerization of MMA and *n*-BA at several monomer feed conditions, catalyzed by CuBr/Me_6TREN. Reaction conditions are given in Table 2.

in the reaction mixture. With these optimizations, copolymers were prepared using this catalyst system. However, the catalyst was still unable to tolerate monomer feed with more than 20% MMA.

For all of the copolymerizations studied, monomer conversion as a function of time and molecular weight evolution as a function of monomer conversion were measured. The molecular weight evolution and molecular weight distributions were first examined to ensure that well-defined copolymers had been prepared. Monomer conversion data were analyzed to show the kinetic behavior of the system. The monomer conversion data were then used to calculate the reactivity ratios of the monomer pair, the cumulative composition of the copolymers, and the instantaneous composition of the copolymers.

Molecular Weights. The molecular weight behaviors of the three catalyst systems are displayed in Figures 1−3. Each figure shows data of three different experiments conducted under different initial monomer feed conditions.

Results of the copolymerizations employing the CuBr/dNbpy catalyst system are given in Figure 1. The initial monomer feed conditions studied in these copolymerizations were 85%, 50%, and 15% (mol) of *n*-BA. As seen in the figure, M_n values of the copolymers increased linearly with cumulative monomer conversion. In all cases, the values are slightly higher than those predicted by theory ($DP_n = \Delta[M]/[I]_0$). The polydispersities of the copolymers decreased throughout the copolymerizations, reaching lowest values of $M_w/M_n \sim 1.2$.

Figure 2 gives the molecular weight data for the copolymerizations using the CuBr/PMDETA catalyst system. The initial monomer feed conditions studied in these copolymerizations were, again, 85%, 50%, and 15% (mol) of *n*-BA. As in the case of the dNbpy copolymerizations, copolymers made using this catalyst system displayed linear increases in M_n values with increasing cumulative monomer conversion. The copolymers had narrow molecular weight distributions, which decreased with increasing conversion reaching values of $M_w/M_n < 1.3$.[20,25] The M_n values observed were slightly higher than what was predicted by theory.

As discussed above, problems with the Me_6TREN catalyst system only allowed study of copolymerizations with low concentrations of MMA in the initial monomer feed. For this reason the data presented in Figure 3 correspond to experiments run with 90%, 85%, and 80% (mol) of *n*-BA. This figure shows that the M_n values of the copolymers increased linearly with conversion and, again, were slightly higher than was predicted by theory. The copolymers had low polydispersities, which decreased with increasing cumulative monomer conversion, reaching values of $M_w/M_n < 1.2$.

Figures 1−3 demonstrate that all copolymers prepared in these experiments have narrow molecular

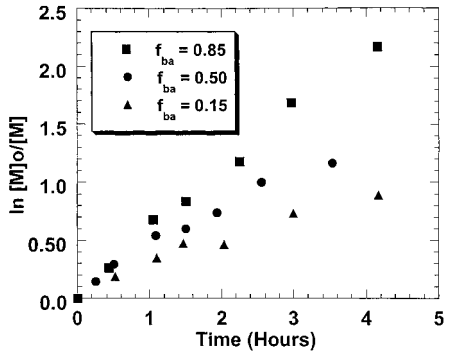

Figure 4. First-order kinetic plot for the copolymerization of MMA and *n*-BA at several monomer feed conditions, catalyzed by CuBr/2dNbpy. Reaction conditions shown in Table 2.

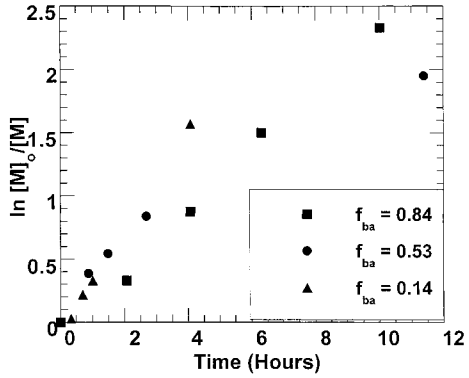

Figure 5. First-order kinetic plot for the copolymerization of MMA and *n*-BA at several monomer feed conditions, catalyzed by CuBr/PMDETA. Reaction conditions shown in Table 2.

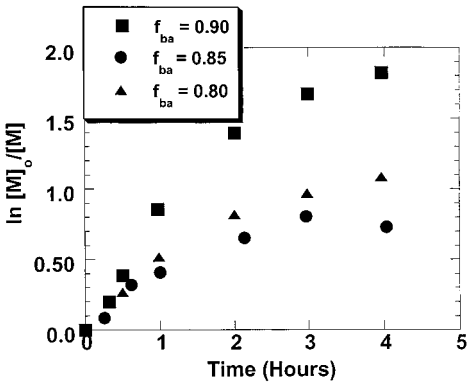

Figure 6. First-order kinetic plot for the copolymerization of MMA and *n*-BA at several monomer feed conditions, catalyzed by CuBr/Me_6TREN. Reaction conditions shown in Table 2.

distributions and M_n values which can be predicted using the equation $DP_n = \Delta[M]/[I]_0$, regardless of the structure of the catalyst used in the copolymerization. In all copolymers studied here, the measured values of molecular weight were slightly and systematically higher than the predicted theory value. It is believed that this observation is due to the fact that M_n values were obtained using GPC calibrated with linear polystyrene standards. The small deviation seen from theory is then attributed to differences in the hydrodynamic volume between MMA/*n*-BA copolymers and linear polystyrene molecules.

Kinetic Data. For the copolymerizations discussed above, monomer conversion as a function of time was also measured. These monomer conversion data are given in Figures 4−7.

The first-order kinetic plots of the copolymerizations carried out using the CuBr/2dNbpy catalyst system are displayed in Figure 4. In this figure it can be seen that, for all three of the copolymerizations, $\ln([M]_0/[M])$ increases linearly with time, indicating that the copolymerizations obey a first-order dependence on total monomer concentration. Two interesting behaviors are observed in Figure 4. First, at high conversions a slight curvature in the increase of $\ln([M]_0/[M])$ can be seen. Second, as the concentration of *n*-BA in the initial monomer feed is increased, the rate of polymerization increases. In the case of the equimolar monomer feed the reactions reached 70% total monomer conversion after 3.6 h. The experiment in which the initial monomer feed contained 85% of *n*-BA reached 90% conversion after 4 h, while the copolymerization with 15% of *n*-BA in the monomer feed reached only 60% conversion after 4 h.

Figure 5 shows the first-order kinetic plots of the three copolymerization conducted in the presence the PMDETA catalyst. This figure shows that $\ln [M]_0/[M]$ increased with time and at short times does so in a generally linear fashion. However, as the time of the reaction increased, some curvature began to occur. This curvature was more significant than in the case of the dNbpy catalyst.

Figure 6 shows the three first-order kinetic plots of the copolymerizations catalyzed by the CuBr/Me_6TREN. In Figure 6 a pronounced curvature in the first-order kinetic plot is observed, and in fact in each case a limiting conversion was reached. This limiting conversion appears to depend on the initial monomer feed composition, and the values fall into a range of 55%−80% of total monomer concentration after 4 h. Similarly to what was observed with the dNbpy system, the rate of polymerization (as well as the limiting conversion) in these reactions increased as the acrylate content of the monomer feed was increased.

The interesting behaviors seen in these results, such as the curvature in the first-order kinetic plots and the rate-enhancing effects of increased *n*-BA, were somewhat unexpected. To better understand and explain these results, a series of computer simulations were carried out on these copolymerizations. The results of these simulations and our explanations of the simulation results are presented in the Discussion section below.

On the basis of the free radical reactivity ratios of MMA and *n*-BA reported in the literature, it is expected that MMA would be consumed more quickly than *n*-BA in these copolymerizations. This is the behavior that was observed in these copolymerizations. An example is shown in Figure 7, which shows individual monomer conversion for the experiment catalyzed by CuBr/2dNbpy using an equimolar monomer feed. After 3.5 h ∼90% of the original MMA had been consumed in comparison to only ∼60% of the *n*-BA. This behavior is typical of what was seen in all of these copolymerizations. These results indicate that the reactivity ratios of this monomer pair follow the same trends that are seen in conventional free radical copolymerizations. The reactivity ratios in these copolymerizations are further discussed below.

Reactivity Ratios. The monomer conversion data shown above were used to calculate the monomer reactivity ratios and 95% joint confidence intervals for the copolymerization of MMA and *n*-BA catalyzed by the three systems studied, using the nonlinear regres-

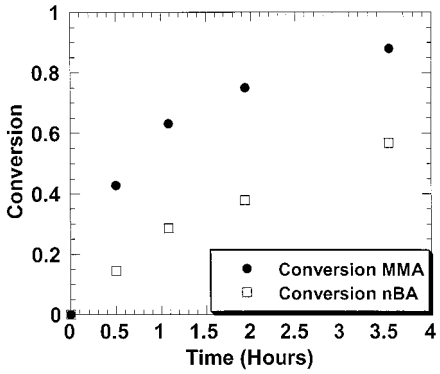

Figure 7. Individual monomer conversion for the copolymerization of MMA and *n*-BA catalyzed by CuBr/2dNbpy. The initial monomer feed in this copolymerization consisted of 50% (mol) *n*-BA. Reaction conditions are given in Table 2.

Table 3. Reactivity Ratios of MMA and *n*-BA from Various Sources

r_{MMA}	r_{BA}	source	r_{MMA}	r_{BA}	source
2.52	0.265	this work (CuBr/dNbpy)	1.88	0.31	ref 33
3.15	0.37	CuBr/PMDETA[20]	2.86	0.11	ref 29
2.07	0.36	CuBr/PMDETA[25]	1.79	0.30	ref 30
1.3	0.35	$NiBr_2/(PPh_3)_2$ [24]	2.06	0.35	ref 31
1.75	0.35	ref 24	2.15	0.26	ref 25

sion techniques described previously.[19] Meaningful data were obtained for the CuBr/dNbpy and CuBr/PMDETA systems; however, no meaningful values were found when the CuBr/Me_6TREN system was analyzed. As mentioned above, there were several problems associated with the copolymerizations using the Me_6TREN catalyst. These problems forced the study of the copolymerization only with monomer feeds that were very high (80%+) in *n*-BA. The intolerance of this catalyst system to higher MMA concentrations prohibited the satisfaction of the Mortimer−Tidwell criteria for the feed conditions required to accurately measure the reactivity ratios of a monomer pair.[46] Since it was impossible to view the appropriate range of feed compositions, the data that were obtained were not meaningful and are therefore not reported here. It is important to note that despite the lack of meaningful reactivity ratios from the copolymerizations using Me_6TREN, the results of these experiments agreed well with the results from the other two catalyst systems. This fact is well demonstrated in the calculations of composition, which are discussed in the following section.

The point estimates of the reactivity ratios of the CuBr/dNbpy and CuBr/PMDETA systems are reported in Table 3 along with several literature values for the ATRP and conventional free radical copolymerization of these two monomers. The table shows acceptable agreement between the literature values and the values that were experimentally determined.

The joint confidence intervals (JCI) and point estimates for the two catalyst systems are shown in Figure 8. The point estimate for the dNbpy catalyst is partially obscured by the JCI of the PMDETA system. This figure shows that there is a fair amount of agreement and overlap in the JCI's of the two catalyst systems. The JCI for the measurements on the dNbpy system is slightly smaller than the JCI for the PMDETA system. This result is consistent with the facts that the reactivity ratios are calculated from conversion data and that the conversion data are more linear and perhaps more reliable in the case of dNbpy.

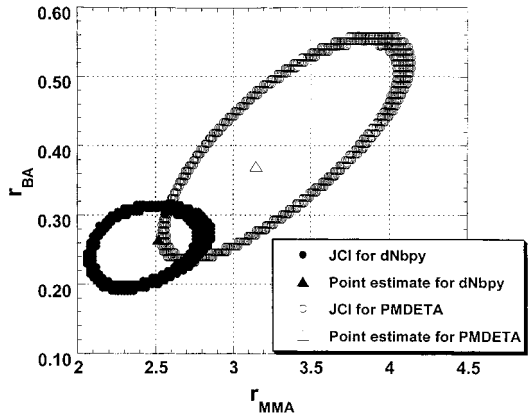

Figure 8. 95% joint confidence intervals and point estimates for the copolymerizaton of MMA and *n*-BA, using Cu(I)Br/PMDETA and Cu(I)Br2/dNbpy.

The results discussed above show a fair amount of agreement between the reactivity ratios calculated for these atom transfer radical copolymerizations and conventional radical polymerizations. This agreement, however, is not perfect. There are several reasons for these discrepancies, which have been discussed previously.[47] Some of the more obvious reasons for these differences are the discrepancies in reaction temperatures and solvent used in conventional radical polymerization as opposed to those used in ATRP. Additionally, differences in the rate of chain growth can also alter the observed reactivity ratios, in that in a controlled polymerization polymer is slowly formed throughout the reaction, whereas in a conventional system high polymer is formed at the beginning of the reaction and the composition of the polymer is established at low conversion. This difference may also lead to a more significant influence of the so-called "bootstrap" effect proposed by Harwood.[48] The presence of a transition metal catalyst in these polymerizations further complicates the picture by introducing the possibility of complexation of some monomers with the weakly Lewis acidic transition metal catalysts. The final, and perhaps most important, cause of discrepancies in reactivity ratios observed in ATRP is the different methods employed to measure reactivity ratios in controlled and conventional radical polymerizations. In a conventional process the monomer reactivity ratios can be measured at low conversion with different monomer feeds; however, in the ATRP process high polymer is not formed immediately in the reaction. Measurements at low conversions could be affected by the structure of the initiator, which may preferentially react with one comonomer. For this reason it is necessary to measure the cumulative composition of the copolymers at a conversion higher than would be studied in a conventional process. However, as the cumulative composition of a copolymer will always be equal to the monomer feed at 100% monomer conversion, the closer the reaction gets to 100% conversion, the less precise information on reactivity ratios can be obtained. In the calculations of reactivity ratios for these copolymerizations, monomer conversion data were used from points as high as 90% total monomer conversion. The results of these calculations demonstrate that these complications do, in fact, affect the reactivity ratios observed for these experiments, but the agreement with literature values shows that these effects are not overwhelming.

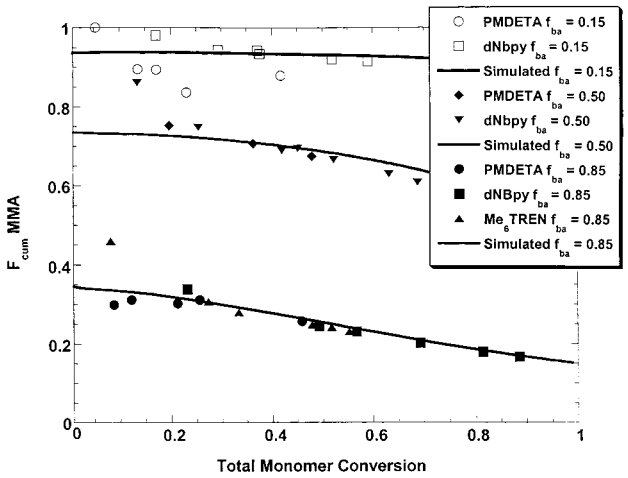

Figure 9. Cumulative copolymer composition vs total conversion of monomer for the copolymerization of MMA and *n*-BA at several monomer feed conditions, catalyzed by CuBr/PMDETA, CuBr/2dNbpy, and CuBr/Me_6TREN. Simulations used $r_{MMA} = 3.0$ and $r_{nBA} = 0.3$; other kinetic parameters are given in Table 1, and reaction conditions are given in Table 2.

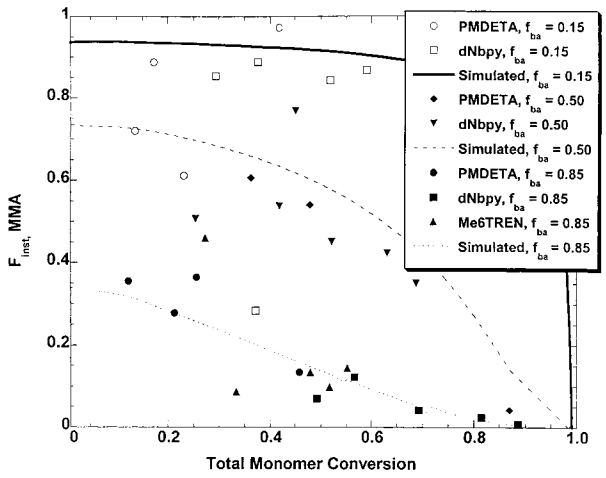

Figure 10. Instantaneous copolymer composition vs total conversion of monomer for the copolymerization of MMA and *n*-BA at several monomer feed conditions, catalyzed by CuBr/PMDETA, CuBr/2dNbpy, and CuBr/Me_6TREN. Simulations used $r_{MMA} = 3.0$ and $r_{nBA} = 0.3$; other kinetic parameters are given in Table 1, and reaction conditions are given in Table 2.

Copolymer Composition. Using the monomer conversion data, cumulative and instantaneous compositions were calculated using eqs 1 and 2.

$$F_{cum,1} = \frac{(\%\ \text{conv})_1[M_1]_0}{(\%\ \text{conv})_1[M_1]_0 + (\%\ \text{conv})_2[M_2]_0} \quad (1)$$

$$F_{inst,1} = F_{cum,1} + (\%\ \text{conv})\frac{\Delta F_{cum,1}}{\Delta(\%\ \text{conv})} \quad (2)$$

The cumulative compositions of copolymers prepared using the three catalyst systems are shown in Figure 9. Because of the limitations of the Me_6TREN, in terms of these copolymerizations, the results of the copolymerization at 85% *n*-BA monomer feed concentration are the only results for this catalyst system shown in Figure 9. This figure demonstrates that the composition of the copolymers is governed only by the initial monomer feed condition used and is independent of the structure of the catalyst system employed. The calculated compositions show good agreement with the values predicted by computer simulation which assumed $r_{MMA} = 3.0$ and $r_{BA} = 0.3$. The exceptions to this generally good agreement are the small deviations seen at low conversions (<25%) in each of these cases. The possible explanations of this low conversion deviation are examined in the Discussion section below. It is important to note the agreement among the results for the three catalyst systems at the low MMA feed condition. It is known that the composition of a copolymer is determined by the monomer feed composition and the reactivity ratios of the monomer pair.[49] For these low MMA feed condition results, the composition of the monomer feed is the same in all reactions; therefore, the fact that the results are very similar implies that the reactivity ratios of the monomers in all three systems must be very similar. This result gives a good indication that the reactivity ratios of this monomer pair in the copolymerizations catalyzed by Me_6TREN is very similar to those in the copolymerizations catalyzed by the other two catalyst systems, despite the fact that it was impossible to measure the reactivity ratio of Me_6TREN directly.

One of the results that was expected from this research was the synthesis of copolymers with significant continuous changes in instantaneous composition (i.e., gradient copolymers). Figure 10 shows the instantaneous compositions corresponding to the cumulative copolymer compositions given in Figure 9. A fair level of agreement among the data from the various systems and the simulated values is demonstrated in this figure. The agreement in the instantaneous composition data is not as good as the agreement in the cumulative composition results. This is an unfortunately unavoidable consequence of the fact that instantaneous composition is calculated from cumulative composition, which in turn is calculated from monomer conversion. For this reason any error in the measurement of conversion will be amplified in the calculation of cumulative composition and further amplified in the calculation of instantaneous composition. Despite this, it is still possible to see that the general trend of the results displayed in Figure 10 is a continuous and significant decrease in the content of MMA in the chain as the length of the chain increases.

Discussion

There were several observations noted in the experiments which were, to some extent, unexpected. Those behaviors were the curvature in the first-order kinetic plots of the copolymerizations, the rate-enhancing effects of increased *n*-BA content in the monomer feed for the dNbpy, and the deviation of experimentally determined compositions from predicted values at low monomer conversion. A series of computer simulations were employed to allow a better understanding of the potential causes of these observations. Each of the three behaviors are discussed below.

To ensure that the conclusions drawn from these simulations are meaningful, it is necessary to compare the results of the simulation with experimental results. To this end, the monomer conversion data shown in Figures 4−6 were plotted with corresponding simulation data. Figure 11 displays the data from Figure 4 and the analogous simulations. Satisfactory agreement between the experimental data and the simulations is observed, as well as the same trends in curvature and rate enhancements with increasing *n*-BA content in the monomer feed. The level of agreement is not as high in

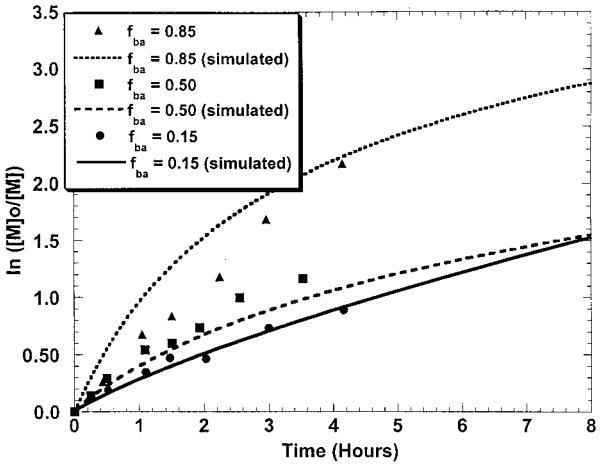

Figure 11. Overlay of first-order kinetic plot data in Figure 4 with results of simulations using the parameters given in Table 1, and $r_{MMA} = 3.0$ and $r_{nBA} = 0.3$. For $f_{ba} = 0.85$ $[MMA]_0 = 1.09$ M, $[BA]_0 = 6.16$ M, $[MBP]_0 = 0.024$ M, and $[Cu(I)]_0 = 0.024$. For $f_{ba} = 0.50$ $[MMA]_0 = 4.00$, $[BA]_0 = 4.00$, $[MBP]_0 = 0.026$, and $[Cu(I)]_0 = 0.026$. For $f_{ba} = 0.15$ $[MMA]_0 = 7.54$, $[BA]_0 = 1.33$, $[MBP]_0 = 0.028$, and $[Cu(I)]_0 = 0.028$.

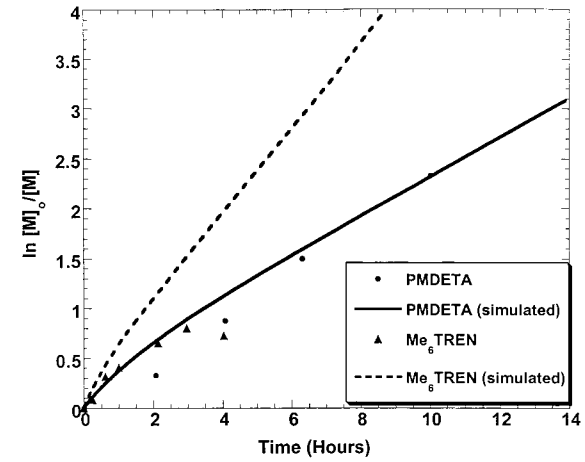

Figure 12. Overlay of first-order kinetic plot data in Figures 5 and 6 with results of simulations using the parameters given in Table 1, $r_{MMA} = 3.0$ and $r_{nBA} = 0.3$, and $[MMA]_0 = 1.09$ M, $[BA]_0 = 6.16$ M, $[MBP]_0 = 0.024$ M, and $[Cu(I)]_0 = 0.024$. For PMDETA catalyst system, $k_{act}(MMA) = 1.5 \times 10^1$ L/mol s, $k_{act}(BA) = 1.5 \times 10^{-1}$ L/(mol s), $k_{deact}(MMA) = 10^7$ L/(mol s), and $k_{deact}(BA) = 8 \times 10^7$. For the Me_6TREN catalyst system, $k_{act}(MMA) = 10^3$ L/(mol s), $k_{act}(BA) = 10^1$ L/(mol s), $k_{deact}(MMA) = 10^7$ L/(mol s), and $k_{deact}(BA) = 8 \times 10^7$.

Figure 12, which is the plot of experimental data from Figures 5 and 6 at 85% MMA in monomer along with the corresponding simulation data. The PMDETA data agree well with the simulated data, but the Me_6TREN experiment follows the simulated data only at low conversion. At higher conversion the experimental data level off at a limiting conversion, but the simulated data do not level and continue in a fairly linear manner. Differences between the experimental and simulated data for the Me_6TREN catalyst system are possibly due to the poor solubility of the catalyst in the reaction mixture.[45] This poor solubility was not taken into account in these simulations. It is important to note that the equilibrium constant used to simulate the PMDETA was only 1.5 times as high as the equilibrium constant for the dNbpy simulations, while normally it is considered to be 10 times higher. This lower value of K_{eq}, however, takes into account the fact that the temperature of the PMDETA copolymerizations was 30 °C lower than that of the dNbpy-catalyzed copolymerizations.

Scheme 2. Schematic Representation of the Establishment of an Equilibrium between Dormant Chains with MMA and BA Terminal Units

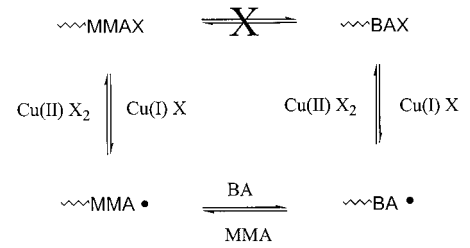

Based on the results illustrated in Figures 11 and 12, the satisfactory agreement between experiment and simulations (especially the dNbpy simulations) suggests that some meaningful conclusions can be made from those simulations. Since it was demonstrated that the simulation models employed gave results that closely resembled the experimentally observed data, these simulation were used to study the concentration of various species that are important to the atom transfer radical copolymerization equilibria illustrated in Scheme 2.

Curvature in Kinetics. In a controlled/living polymerization curvature at high conversion in a first-order kinetics plot is typically indicative of irreversible termination. However, the final polydispersity values in these experiments were between $M_w/M_n = 1.3$ and $M_w/M_n = 1.1$, implying that the contribution of termination in these copolymerizations is not very significant. This suggests that some factor other than irreversible termination could be responsible for the observed curvature.

Figure 13a−c shows the evolution of concentrations of dormant polymer chains with MMA and *n*-BA ultimate units (MMAX and BAX), active polymers chains with MMA and *n*-BA ultimate units (MMA* and BA*), Cu(I)Br, and Cu(II)Br_2 (the amount of the $CuBr_2$ formed is equal to the concentration of dead chains) for the three copolymerizations catalyzed by copper complexed by dNbpy. Several important results are noticed in Figure 13a−c. First, in each plot it is seen that early in the reactions (<5% conversion) a certain level of [Cu(II)Br_2] is established. This level of [Cu(II)Br_2] remains essentially constant until very high monomer conversion is reached. Second, this plateau of [Cu(II)Br_2] gets progressively larger as the concentration of *n*-BA is decreased. The copolymerization that began with 85% *n*-BA converted 0.8% of catalyst to Cu(II), the 50% *n*-BA reaction converted 2.2% of Cu(I) to Cu(II), and the copolymerization with 15% *n*-BA in the initial monomer feed reached 4.0% Cu(II). Finally, these figures show that the radical concentrations in these copolymerizations display different behavior. As expected, based on the reactivity ratios of the monomer pair, [MMA*] is high at the beginning of the reaction and then decreases as MMA monomer is consumed. As the amount of *n*-BA in the initial monomer feed is increased, the rate of the decrease in [MMA*] becomes faster, and final [MMA*] gets lower.

During an atom transfer radical (co)polymerization, the concentration of Cu(II) generated is determined by the total radical concentration, as illustrated in Scheme 2. Early in these copolymerizations when a plateau concentration of Cu(II) is reached, a nearly steady [BA*]

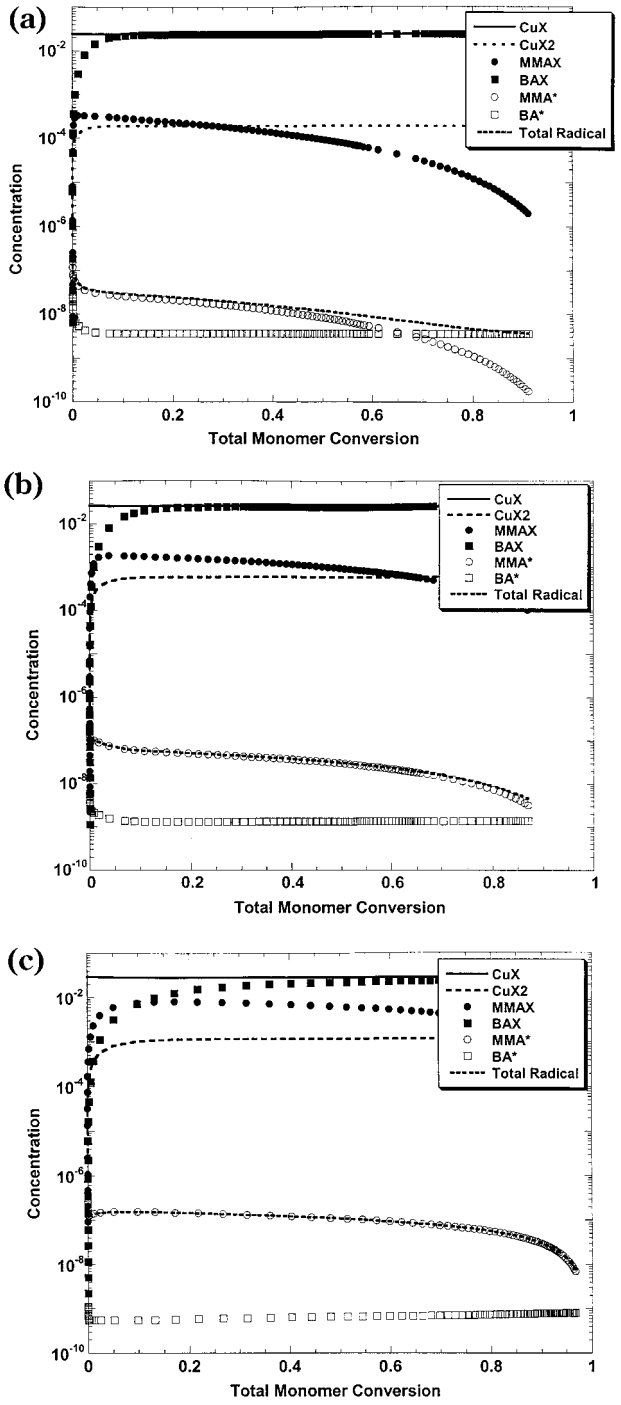

Figure 13. Concentrations of various species vs total conversion of monomer for simulated data, using the kinetic parameters given in Table 1, and $r_{MMA} = 3.0$ and $r_{nBA} = 0.3$. (a) $f_{ba} = 0.85$, $[MMA]_0 = 1.09$ M, $[BA]_0 = 6.16$ M, $[MBP]_0 = 0.024$ M, and $[Cu(I)]_0 = 0.024$. (b) $f_{ba} = 0.50$, $[MMA]_0 = 4.00$, $[BA]_0 = 4.00$, $[MBP]_0 = 0.026$, and $[Cu(I)]_0 = 0.026$. (c) $f_{ba} = 0.15$, $[MMA]_0 = 7.54$, $[BA]_0 = 1.33$, $[MBP]_0 = 0.028$, and $[Cu(I)]_0 = 0.028$.

is achieved. Figure 13 shows that while the [BA*] remains nearly constant, until high monomer conversion, the concentration of the less reactive [MMA*] decreases significantly at high monomer conversions. This decrease in [MMA*] happens more quickly, and the final [MMA*] reaches a lower value, in reactions that have a higher initial *n*-BA concentration. This also leads to the more pronounced curvature of semilogarithmic plots. At the same time, since BA* are much more

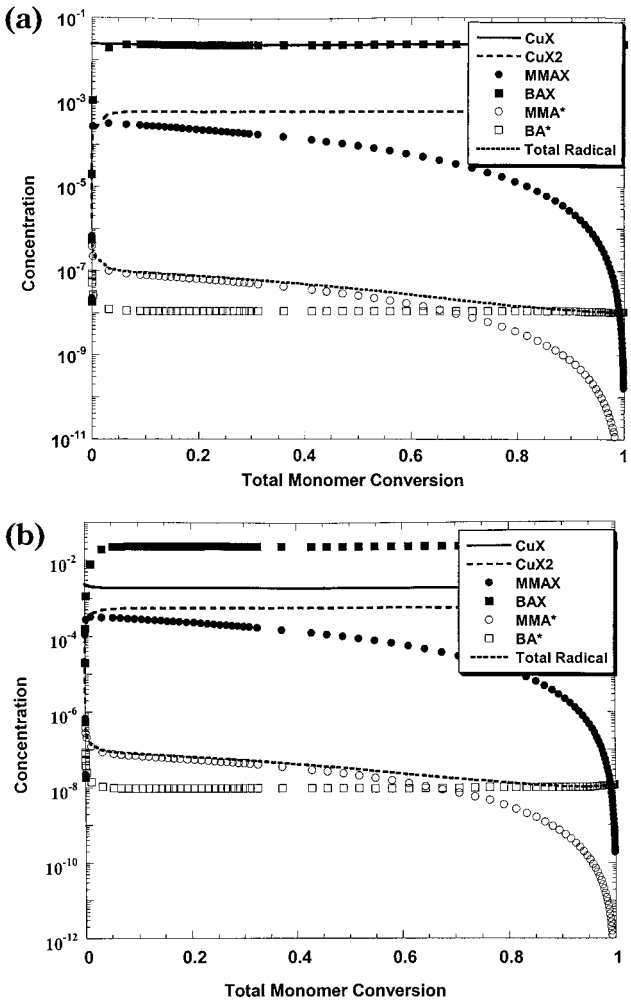

Figure 14. Concentrations of various species vs total conversion of monomer for simulated data, using the kinetic parameters given in Table 1, and $[MMA]_0 = 1.09$ M $[BA]_0 = 6.16$ M, $[MBP]_0 = 0.024$ M, and $[Cu(I)]_0 = 0.024$. Simulations used $r_{MMA} = 3.0$ and $r_{nBA} = 0.3$. (a) Copolymerization modeling the PMDETA catalyst system, $k_{act}(MMA) = 1.5 \times 10^1$ L/(mol s), $k_{act}(BA) = 1.5 \times 10^{-1}$ L/(mol s), $k_{deact}(MMA) = 10^7$ L/(mol s), and $k_{deact}(BA) = 8 \times 10^7$. (b) Copolymerization modeling the Me_6TREN catalyst system, $k_{act}(MMA) = 10^3$ L/(mol s), $k_{act}(BA) = 10^1$ L/(mol s), $k_{deact}(MMA) = 10^7$ L/(mol s), and $k_{deact}(BA) = 8 \times 10^7$.

reactive than MMA*, the overall rate is higher at higher $[BA]_0$ despite much lower [MMA*].

Figure 14a,b gives the simulated concentrations for the PMDETA and Me_6TREN catalyst systems at low initial $[n\text{-BA}]_0$. These figures demonstrate that the concentrations in these simulations exhibit many of the same behaviors as observed in the dNbpy simulations. In these simulations it is again noticed that a plateau concentration of Cu(II) is reached very early in the reaction. The decrease in [MMA*] with increasing conversion is seen in these figures as well.

Figures 13 and 14 show that copolymerizations exhibit not only a decrease in [MMA*] but also a decrease in total radical concentration with total monomer conversions. Comparing the results given in Figures 11 and 12 with those given in Figures 13 and 14 leads to the observation that the copolymerizations, which display the highest level of curvature, are also the ones with the most significant drop in total radical concentration.

The figures discussed above clearly point to the total and relative radical concentrations as the major factors

in the curvature in the first-order kinetic plots and the effects, on rate, of the composition of the initial monomer feed.

Equilibration Dynamics. At sufficiently high conversion (above 25%), the cumulative and instantaneous compositions plotted in Figures 8 and 9 display good agreement of the experimental points with values predicted by computer simulation. At lower conversions, however, there are some deviations from the predicted behavior. Two possible causes of these deviations have been identified. First, it has been previously reported that GC measurements at very low monomer conversion are subject to larger errors than measurements made at higher conversions.[19] As the compositions reported in this paper are calculated from monomer conversion, those errors will be reflected in the plots of copolymer composition. The other possibility is that the system equilibrates slowly and is not yet at equilibrium when these lower conversion points are measured, as recently suggested.[26]

In an atom transfer radical copolymerization, the two halogen-capped dormant species should interconvert. This interconversion cannot be established directly and instead must be established through a series of equilibria, as described in Scheme 2.

The cross-propagation equilibrium between the two active species is established when the product of the rate constant of addition of MMA to *n*-BA* (k_{BM}) times [MMA] times [*n*-BA*] becomes equal to the rate constant of addition of *n*-BA to a MMA* (k_{MB}) times [*n*-BA] times [MMA*]. Equation 3 gives these two expressions and sets the quotient equal to a number N_{cp}, which will equal unity when the cross-propagation is at equilibrium.

$$\frac{(k_{BM})[MMA][BA^*]}{(k_{MB})[MMA^*][BA]} = N_{cp} \qquad (3)$$

Measurements of monomer conversion made before this equilibrium is reached will give values that are not entirely meaningful. In contrast, measurements made after this equilibrium has been established will be accurate reflections of the true behavior of the system. For this reason, it is important to know how long it takes for this equilibrium to be established.

Similar expressions can be derived for the two other equilibria shown in Scheme 2. They are given below in eqs 4 and 5. Again, in these systems, when the quotient reaches a value of unity, the exchange between BA chain ends (N_{eB}) and MMA chain ends (N_{eM}) is at equilibrium, respectively.

$$\frac{(k_{act,BA})[BAX][Cu(I)X]}{(k_{deact,BA})[BA^*][Cu(II)X_2]} = N_{eB} \qquad (4)$$

$$\frac{(k_{act,MMA})[MMAX][Cu(I)X]}{(k_{deact,MMA})[MMA^*][Cu(II)X_2]} = N_{eM} \qquad (5)$$

The value of quotients in eqs 3−5 and the concentration of initiator (RX) are plotted in Figure 15 for the simulation of the copolymerizations catalyzed by the CuBr/2dNbpy, 85% *n*-BA in the initial monomer feed. It can be seen from these plots that the cross-propagation equilibrium and the MMA activation/deactivation equilibrium are established almost instantaneously. The *n*-BA activation/deactivation equilibrium, however, is established much more slowly. It appears that the reasons for this are centered on the fact that the initiator has the same reactivity as the *n*-BA monomer. The amount of Br atoms in this system must be constant throughout the reaction, but the distribution of these Br atoms among MMA chain ends, *n*-BA chain ends, and initiating alkyl groups does not remain constant. The cross-propagation equilibrium and the MMA activation/deactivation equilibrium are established quickly because they can come to this equilibrium on their own, while *n*-BA, on the other hand, must depend also on the initiator concentration as the two molecules have the same reactivities. It can be seen in Figure 15 that the *n*-BA activation/deactivation equilibrium is established at the same time that the initiator is completely consumed. This happens at approximately 20% monomer conversion. At this point the *n*-BA activation/deactivation equilibrium is no longer influenced by the presence of initiator molecules with the same reactivity.

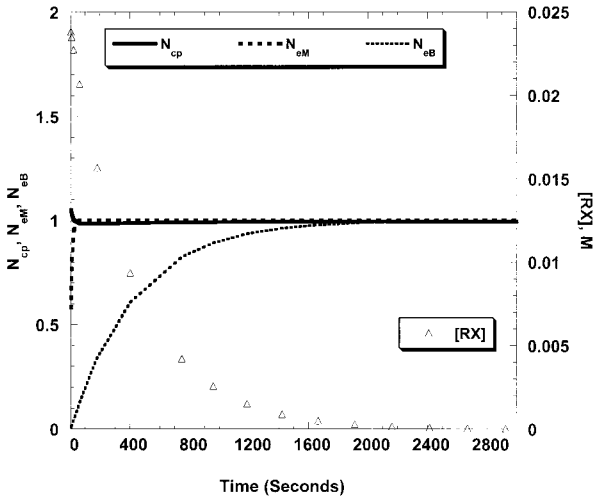

Figure 15. Values of the quotients (eqs 3−5) describing the establishment of the equilibria between active and dormant species as a function of time. The kinetic parameters were taken from Table 1; $r_{MMA} = 3.0$, $r_{nBA} = 0.3$; $f_{ba} = 0.85$ ($[MMA]_0 = 1.09$ M, $[BA]_0 = 6.16$ M); $[MBP]_0 = 0.024$ M; $[Cu(I)]_0 = 0.024$ M.

Despite the slow establishment of the *n*-BA activation/deactivation equilibrium, it is clear that cross-propagation equilibrium is established almost instantaneously. The compositions of the copolymers studied are dependent only on this cross-propagation equilibrium. On the basis of this, it seems that any deviations in composition calculations should not be due to the slow establishment of the cross-propagation equilibrium but more likely caused by either experimental errors in the measurement of monomer conversion or changes in monomer/radical reactivities by for example complexation with a catalyst.

Conclusions

It has been demonstrated that atom transfer radical copolymerization of methyl methacrylate and *n*-butyl acrylate can be performed with three Cu(I)-based catalyst systems. The molecular weights of these copolymers agreed well with theory, and their molecular weight distributions were narrow. The copolymerizations displayed fairly linear first-order kinetic plots, and it was demonstrated that the curvature witnessed in some of these first-order kinetic plots is caused by the decrease in total radical concentration at higher total monomer

conversion. It was observed that some copolymerization displayed an increased rate with increased *n*-BA content in the initial monomer feed. The results of a series of simulated reactions have shown that this effect could be explained by the relative concentration of MMA and *n*-BA radicals. Reactivity ratios were calculated for the monomer pair and were found to be in good agreement with literature values reported for the conventional free radical copolymerization of this monomer pair. Cumulative and instantaneous compositions of the copolymers were calculated and were found to agree well with predicted values. The dynamics of the equilibration of the copolymerizations was investigated in an effort to explain some small deviations in calculated values of composition. These investigations have demonstrated that the cross-propagation equilibrium is established very quickly and does not interfere with the observed values of composition. Reactivity ratios and copolymer compositions were found to be independent of catalyst system used, further suggesting that all copolymerizations studied proceed through the same free radical mechanism.

Acknowledgment. The authors acknowledge Scott G. Gaynor and Stephen V. Arehart for helpful discussions. The ATRP Consortium at Carnegie Mellon University and the Department of the Army (AASERT Contract DAA655-97-1-0191) are acknowledged for their partial financial support of this research.

References and Notes

(1) Matyjaszewski, K., Ed. *Controlled/Living Radical Polymerization: Progress in ATRP, NMP, and RAFT*; American Chemical Society: Washington, DC, 2000.
(2) Matyjaszewski, K., Ed. *Controlled Radical Polymerization*; American Chemical Society: Washington, DC, 1998.
(3) Patten, T. E.; Matyjaszewski, K. *Acc. Chem. Res.* **1999**, *32*, 895.
(4) Patten, T. E.; Matyjaszewski, K. *Adv. Mater.* **1998**, *12*, 901.
(5) Sawamoto, M.; Kamigaito, M. *CHEMTECH* **1999**, *29*.
(6) Matyjaszewski, K. *Chem. Eur. J.* **1999**, *5*, 3095.
(7) Matyjaszewski, K.; Shipp, D. A.; McMurtry, G. P.; Gaynor, S. G.; Pakula, T. *J. Polym. Sci., Part A* **2000**, *38*, 2023.
(8) Shipp, D. A.; Wang, J.-L.; Matyjaszewski, K. *Macromolecules* **1998**, *31*, 8005.
(9) Sedjo, R. A.; Mirous, B. K.; Brittain, W. J. *Macromolecules* **2000**, *33*, 1492.
(10) Gaynor, S. G.; Matyjaszewski, K. *Polym. Mater. Sci. Eng.* **1998**, *79*, 128.
(11) Zhang, X.; Xia, J.; Matyjaszewski, K. *Macromolecules* **2000**, *33*, 2340.
(12) Hedrick, J. L.; Trollsas, M.; Hawker, C. J.; Arthoff, B.; Claesson, H.; Hiese, A.; Miller, R. D.; Mercerreyes, D.; Jerome, R.; Dubois, P. *Macromolecules* **1998**, *31*, 8691.
(13) Kryszewski, M. *Polym. Adv. Technol.* **1997**, *8*, 244.
(14) Pakula, T.; Matyjaszewski, K. *Macromol. Theory Simul.* **1996**, *5*, 987.
(15) Greszta, D.; Matyjaszewski, K. *Polym. Prep. (Am. Chem. Soc., Polym. Div.)* **1996**, *37* (2), 569.
(16) Matyjaszewski, K.; Ziegler, M. J.; Arehart, S. V.; Greszta, D.; Pakula, T. *J. Phys. Org. Chem.* **2000**, *13*, 775.
(17) Greszta, D.; Matyjaszewski, K.; Pakula, T. *Polym. Prepr. (Am. Chem. Soc., Div. Polym. Chem.)* **1997**, *38* (1), 709.
(18) Arehart, S. V.; Greszta, D.; Matyjaszewski, K. *Polym. Prepr. (Am. Chem. Soc., Div. Polym. Chem.)* **1997**, *38* (1), 705.
(19) Arehart, S. V.; Matyjaszewski, K. *Macromolecules* **1999**, *32*, 2221.
(20) Arehart, S. V.; Matyjaszewski, K. *Polym. Prepr. (Am. Chem. Soc., Div. Polym. Chem.)* **1999**, *40* (2), 458.
(21) Haddleton, D. M.; Crossman, M. C.; Hunt, K. H.; Topping, C.; Waterson, C.; Suddaby, K. G. *Macromolecules* **1997**, *30*, 3992.
(22) Kotani, Y.; Kamigaito, M.; Sawamoto, M. *Macromolecules* **1998**, *31*, 5582.
(23) Uegaki, H.; Kontani, Y.; Kamigaito, M.; Sawamoto, M. *Macromolecules* **1998**, *31*, 6756.
(24) Moineau, G.; Minet, M.; Dubois, P.; Teyssie, P.; Senninger, T.; Jerome, R. *Macromolecules* **1999**, *32*, 27.
(25) Roos, S. G.; Muller, A. H. E.; Matyjaszewski, K. *Macromolecules* **1999**, *32*, 8331.
(26) Chambard, G.; Klumperman, B. *ACS Symp. Ser.* **2000**, *768*, 197.
(27) Matyjaszewski, K.; Nakagawa, Y.; Jasieczek, C. B. *Macromolecules* **1998**, *31*, 1535.
(28) Wang, J.-L.; Grimaud, T.; Matyjaszewski, K. *Macromolecules* **1997**, *30*, 6507.
(29) Brosse, J. C.; Gauthier, J. M.; Lenain, J. C. *Makromol. Chem.* **1983**, *184*, 505.
(30) Dube, M. A.; Penlidis, A. *Polymer* **1995**, *36*, 587.
(31) Madruga, E. L.; Fernandez-Garcia, M. *Macromol. Chem. Phys.* **1996**, *197*, 3743.
(32) Hadda, T. B.; Bozec, H. L. *Polyhedron* **1988**, *7*, 575.
(33) Hakim, M.; Verhoeven, V.; McManus, N. T.; Dube, M. A.; Penlidis, A. *J. Appl. Polym. Sci.* **2000**, *77*, 602.
(34) Greszta, D.; Matyjaszewski, K. *J. Polym. Sci., Polym. Chem.* **1997**, *35*, 1857.
(35) Shipp, D. A.; Matyjaszewski, K. *Macromolecules* **1999**, *32*, 2948.
(36) Shipp, D. A.; Matyjaszewski, K. *Macromolecules* **2000**, *33*, 1553.
(37) Matyjaszewski, K.; Patten, T. E.; Xia, J. *J. Am. Chem. Soc.* **1997**, *119*, 674.
(38) Ciampolini, M.; Nardi, N. *Inorg. Chem.* **1966**, *5*, 41.
(39) Wulkow, M. *Macromol. Theory Simul.* **1996**, *5*, 393.
(40) Davis, K. A.; Paik, H.-j.; Matyjaszewski, K. *Macromolecules* **1999**, *32*, 1767.
(41) Matyjaszewski, K. *Macromolecules* **1999**, *32*, 9051.
(42) Walbiner, M.; Wu, J. Q.; Fischer, H. *Helv. Chim. Acta* **1995**, *78*, 910.
(43) Xia, J.; Matyjaszewski, K. *Macromolecules* **1997**, *30*, 7697.
(44) Xia, J.; Gaynor, S. G.; Matyjaszewski, K. *Macromolecules* **1998**, *31*, 5958.
(45) Queffelec, J.; Gaynor, S.; Matyjaszewski, K. *Macromolecules* **2000**, *33*, 8629.
(46) Tidwell, P. W.; Mortimer, G. A. *J. Polym. Sci.* **1965**, *3*, 369.
(47) Matyjaszewski, K. *Macromolecules* **1998**, *31*, 4170.
(48) Harwood, H. J. *Macromol. Symp.* **1987**, *10/11*, 331.
(49) Mayo, F. R.; Lewis, F. M. *J. Am. Chem. Soc.* **1944**, *66*, 1594.

MA001182K